Supplementary Information for

The protein phosphatase 2C domain contributes to the pathobiological function of adenylyl cyclase in *Cryptococcus neoformans*

Soojin Yu[1*], Seong-Ryong Yu[1*], Myung Kyung Choi[2*], Jae-Hyung Jin[1*], Vikas Yadav[3*], Hee Seong Choi[2], Eui-Seong Kim[4], Hyun-Woo Kim[4], Jae-Seok Jeong[4], Do-Kyun Kim[4], Joseph Heitman[3], Hyun-Soo Cho[2], Kyung-Tae Lee[4], and Yong-Sun Bahn[1]

[1]Department of Biotechnology, College of Life Science and Biotechnology, Yonsei University, Seoul 03722, Republic of Korea

[2]Department of Systems Biology, College of Life Science and Biotechnology, Yonsei University, Seoul 03722, Republic of Korea

[3]Department of Molecular Genetics and Microbiology, Duke University Medical Center, Durham, NC 27710, USA

[4]Korea Zoonosis Research Institute, Jeonbuk National University, Iksan 54531, Republic of Korea

This PDF file includes:

Supplementary figures 1-13

Supplementary tables 1-2

Supplementary notes 1-7

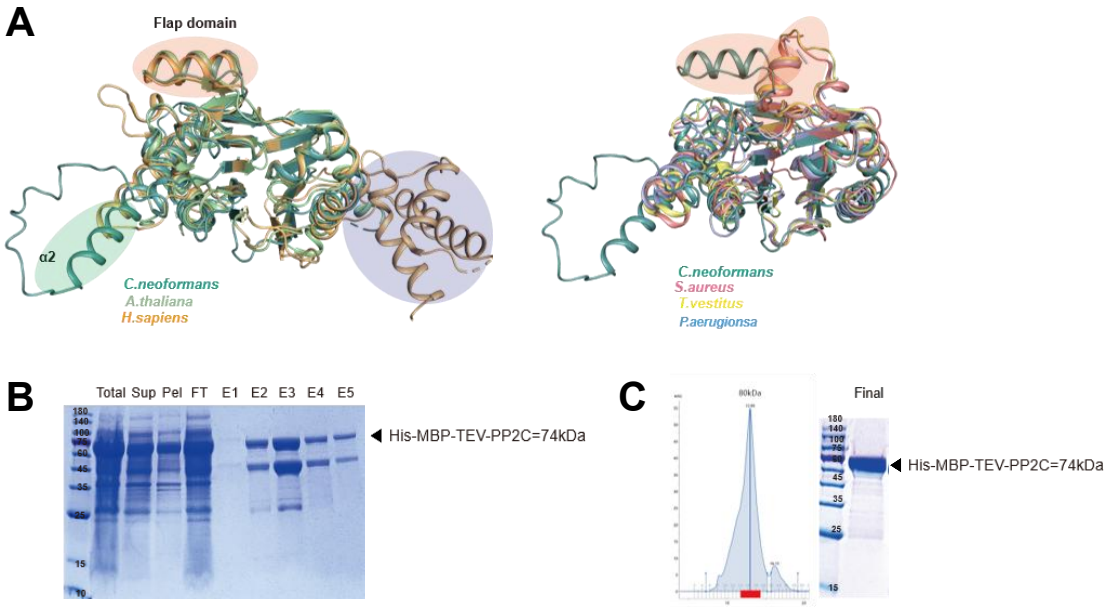

Supplementary figure 1. (A) Structural alignment of PP2C like domains. Overall PP2C fold were similar except flap domain (orange circle) and additional α2 helix (green circle) and missing the additional three alpha-helices at the C-terminus (purple circle). (green: *C. neoformans*, light green: *A. thaliana*, yellow: *H. sapiens*, lime: *T. vestitus*, blue: *P. aeruginosa*, salmon: *S.aureus*) (B) Coomassie blue stained SDS-PAGE gel of the Ni-affinity purified Cac1-PP2C domain. (C) Size exclusion chromatography and Coomassie blue stained SDS-PAGE gel of the purified PP2C domain.

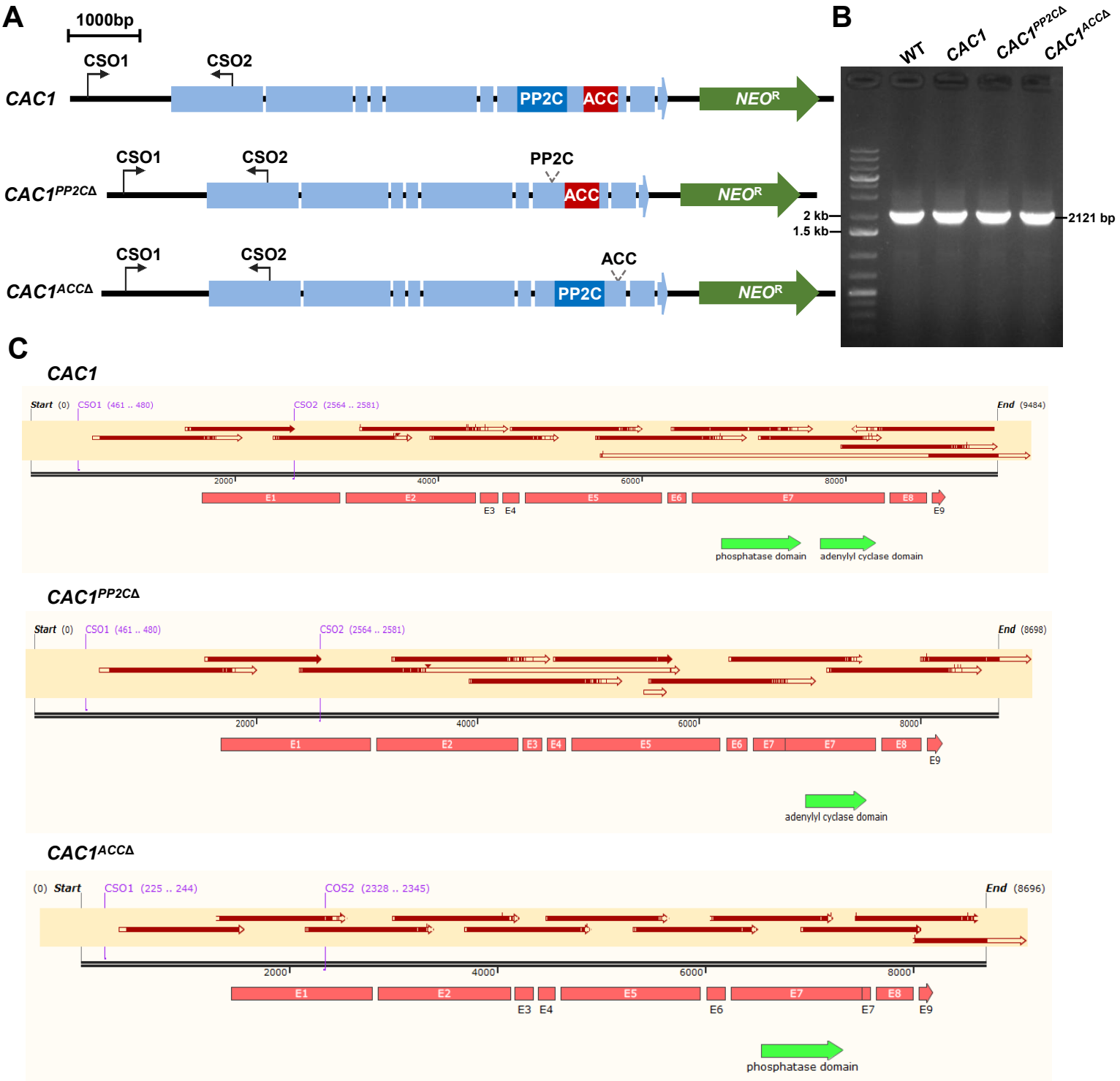

Supplementary Figure 2. Construction of domain deletion and complementation strains were confirmed through sequencing and diagnostic PCR. A) Graphical representation of domains, deletion sites, and primer binding sites. B) Diagnostic PCR was performed to confirm the targeted integration of *CAC1*, *CAC1*$^{PP2C\Delta}$, and *CAC1*$^{ACC\Delta}$ alleles into the native locus of *CAC1*. CSO1 and CSO2 primers were used, and expected band size is 2121 bp. C) Each *CAC1*, *CAC1*$^{PP2C\Delta}$, and *CAC1*$^{ACC\Delta}$ allele was confirmed through sequencing.

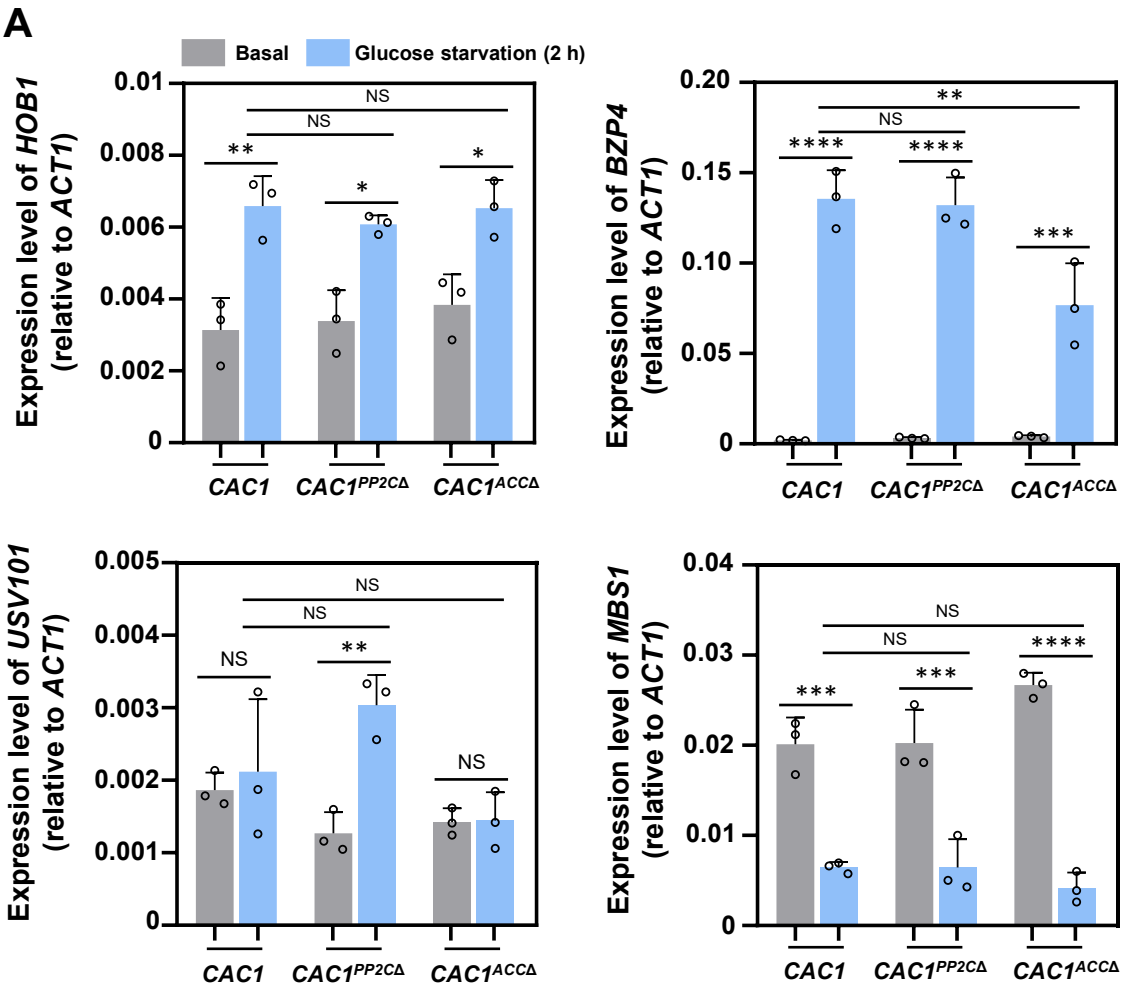

Supplementary Figure 3. Expression of melanin-regulating genes were measured after glucose starvation. A) Quantitative RT-PCR was performed using total RNA of each strain under nutrient rich (basal; YPD; shown in grey) or glucose starvation (YNB without amino acid and glucose; shown in blue) conditions. The expression levels of *HOB1*, *BZP4*, *USV101*, and *MBS1* were measured in *CAC1*, *CAC1*$^{PP2C\Delta}$, and *CAC1*$^{ACC\Delta}$ strains. Three biological replicates were performed with three technical replicates each, and the expression level of each gene was normalized to *ACT1* (ΔCt). Error bars indicate SEM, and statistical analysis was performed by one-way ANOVA multiple comparisons with Tukey's multiple comparison test (*, $P < 0.05$; **, $P < 0.01$; ***, $P < 0.001$; ****, $P < 0.0001$; NS, not significant).

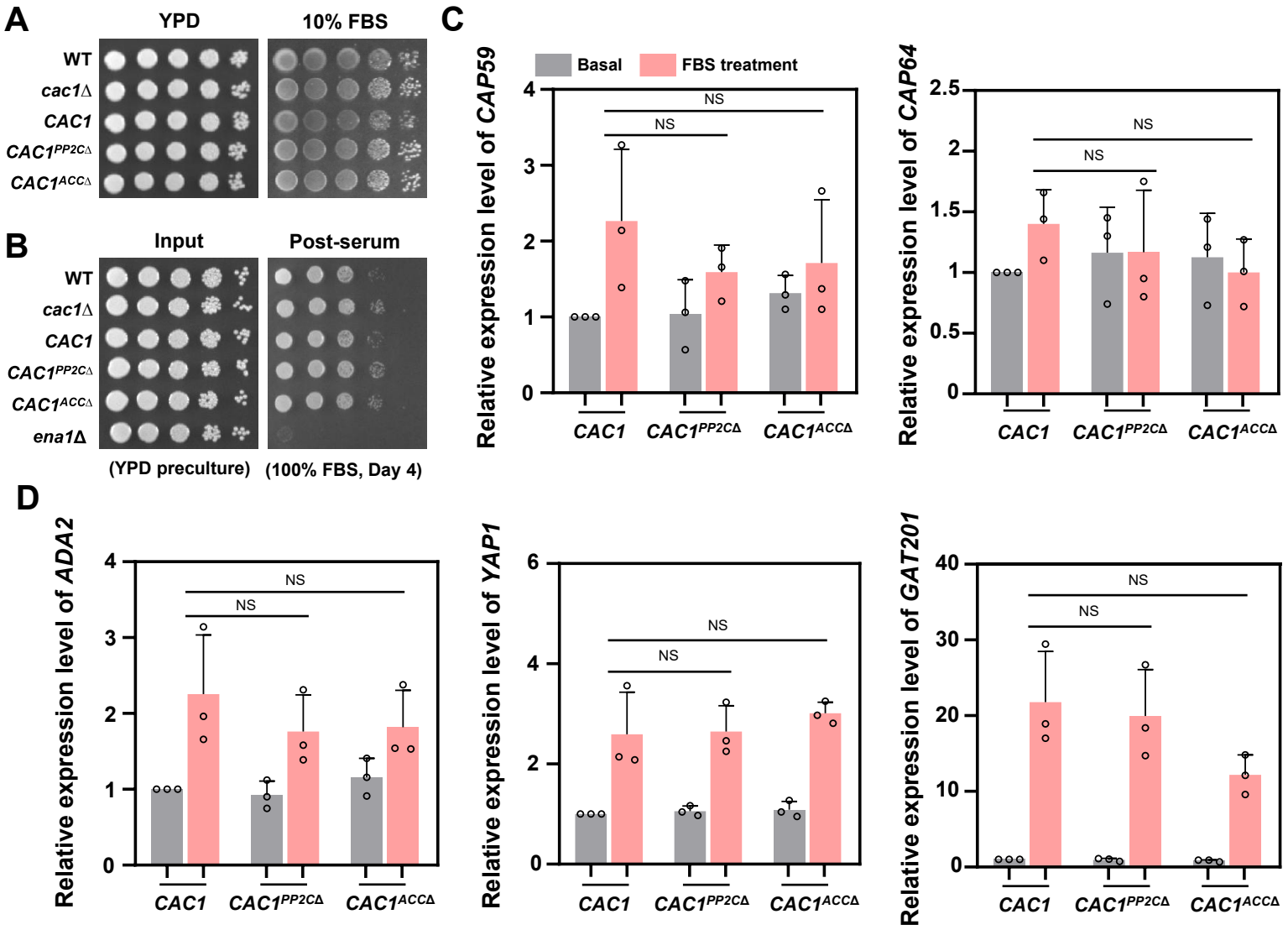

Supplementary Figure 4. Growth and expression analyses were performed after FBS treatment. (A) Spot dilution assay of indicated strains on YPD or 10% FBS agar media identical to the media used for FBS capsule analysis. The indicated strains were grown in liquid YPD for 16 h, washed with sterile PBS, serially diluted 10-fold, and spotted onto YPD or 10% FBS agar plates. The plates were incubated at 37°C and imaged after 3 days. (B) Serum survival assay of indicated cells before and after incubation in 100% FBS for 4 days. The indicated strains were grown in liquid YPD for 16 h, washed with sterile PBS, serially diluted 10-fold, and spotted onto YPD agar plates as the input. Next, the washed cells were 1/10 diluted into 100% heat-inactivated FBS. The cells were then incubated at 37°C with shaking for 4 days, serially diluted 10-fold, and spotted onto YPD agar plates. Both input and post-serum plates were incubated at 30°C for 2 days and imaged. (C) Quantitative RT-PCR was performed using total RNA of each strain under nutrient rich (basal; YPD; shown in grey) or 10% FBS induction condition for 6 h (shown in pink). The expression levels of *CAP59* and *CAP64* were measured in *CAC1*, *CAC1*$^{PP2C\Delta}$, and *CAC1*$^{ACC\Delta}$ strains. (D) Quantitative RT-PCR was performed using total RNA of each strain under nutrient rich (basal; YPD; shown in grey) or 10% FBS condition for 2h (shown in pink). The expression levels of *ADA2*, *YAP1*, and *GAT201* were measured in *CAC1*, *CAC1*$^{PP2C\Delta}$, and *CAC1*$^{ACC\Delta}$ strains. Three biological replicates were performed with three technical replicates each, and relative transcript levels were calculated using the $2^{-\Delta\Delta Ct}$ method. Error bars indicate SEM, and statistical analysis was performed by one-way ANOVA multiple comparisons with Tukey's multiple comparison test (*, $P < 0.05$; **, $P < 0.01$; ***, $P < 0.001$; ****, $P < 0.0001$; NS, not significant).

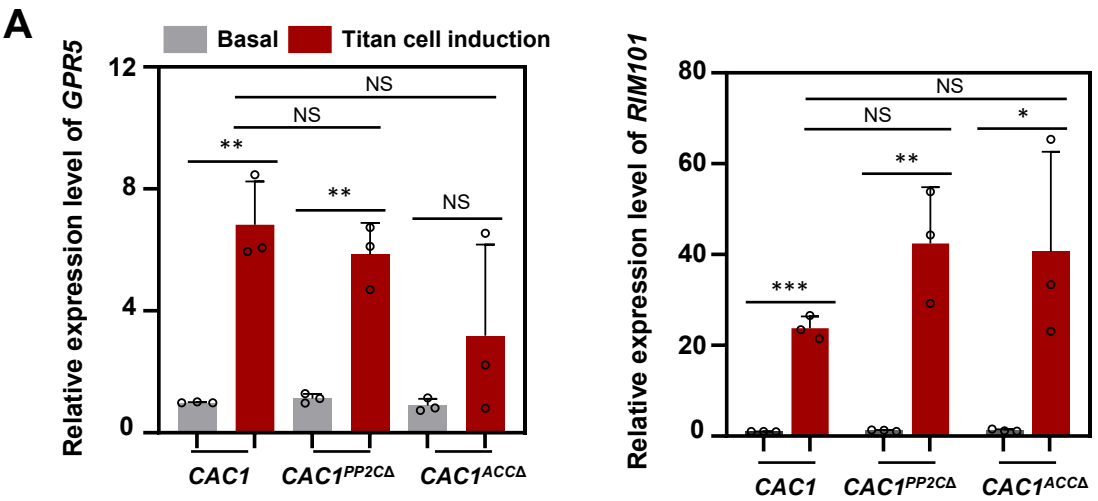

Supplementary Figure 5. Expression of titan cell-regulating genes were measured after titan cell induction. A) Quantitative RT-PCR was performed using total RNA of each strain under nutrient rich (basal; YPD; shown in grey) or titan cell induction condition (shown in red; condition detailed in materials and methods). The expression levels of *GPR5* and *RIM101* were measured in *CAC1*, *CAC1*$^{PP2C\Delta}$, and *CAC1*$^{ACC\Delta}$ strains. Three biological replicates were performed with three technical replicates each, and relative transcript levels were calculated using the $2^{-\Delta\Delta Ct}$ method. Error bars indicate SEM, and statistical analysis was performed using an unpaired two-tailed Student's t-test (*, $P < 0.05$; **, $P < 0.01$; ***, $P < 0.001$; ****, $P < 0.0001$; NS, not significant).

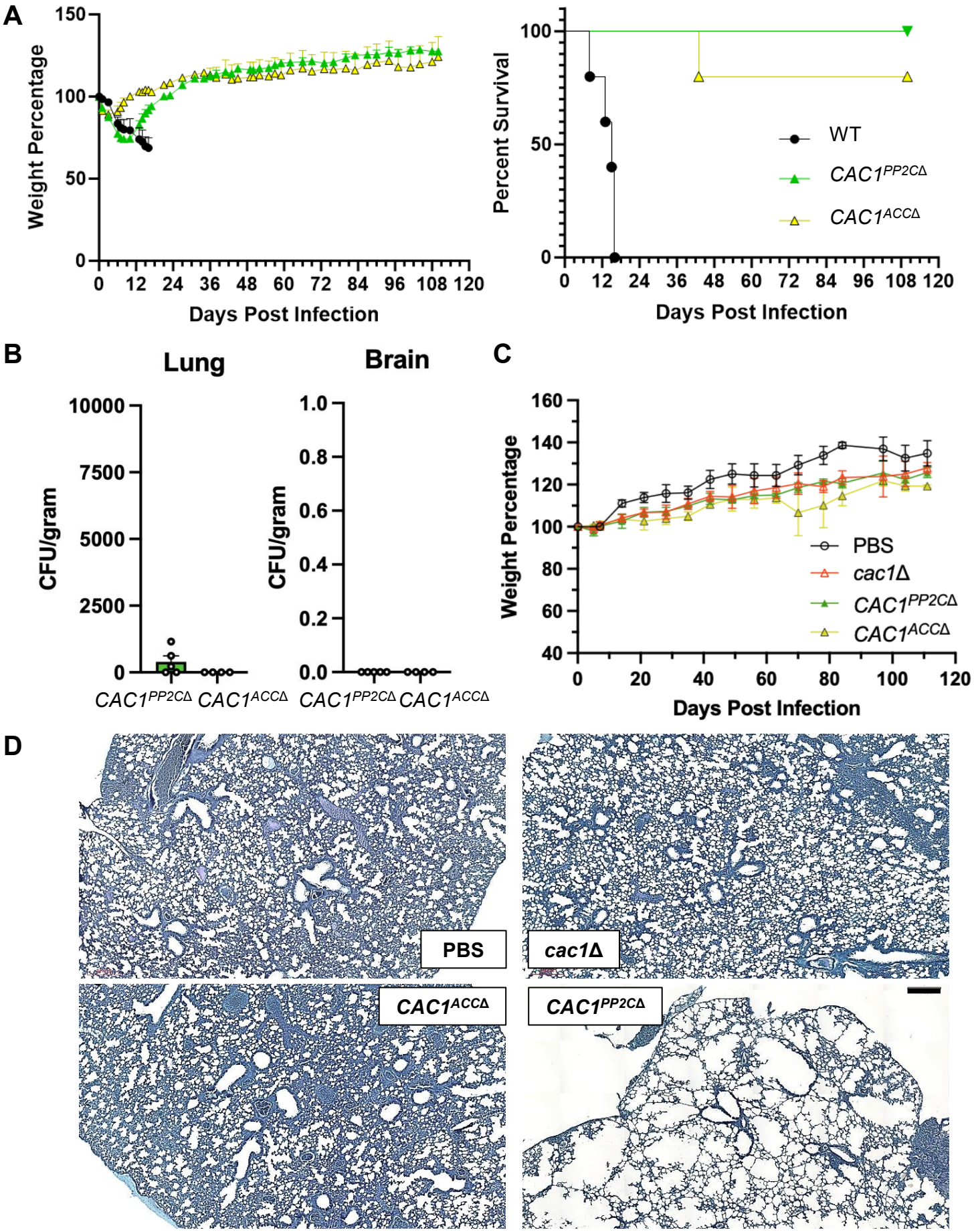

Supplementary Figure 6. Long-term survival analysis. Balb/c mice were infected intranasally with 5 × 10^5 cells of *Cryptococcus neoformans* strains and sacrificed for each analysis. (A-B) Long-term survival assay (n=5). Body weight changes of infected mice and survival curves analyzed by the log-rank (Mantel–Cox) test, with corresponding *P*-values: WT vs *CAC1*$^{PP2C\Delta}$ (0.0027); WT vs *CAC1*$^{ACC\Delta}$ (0.0027). (B) Fungal burden (colony-forming units) in lung and brain tissues was determined at 111 days post-infection. (C-D) Additional cohort (n=2) used for histopathological analysis. Body weight changes of these mice (C) and corresponding lung sections stained with PAS at 111 dpi (D) are shown. Scale bar indicates 200 μm.

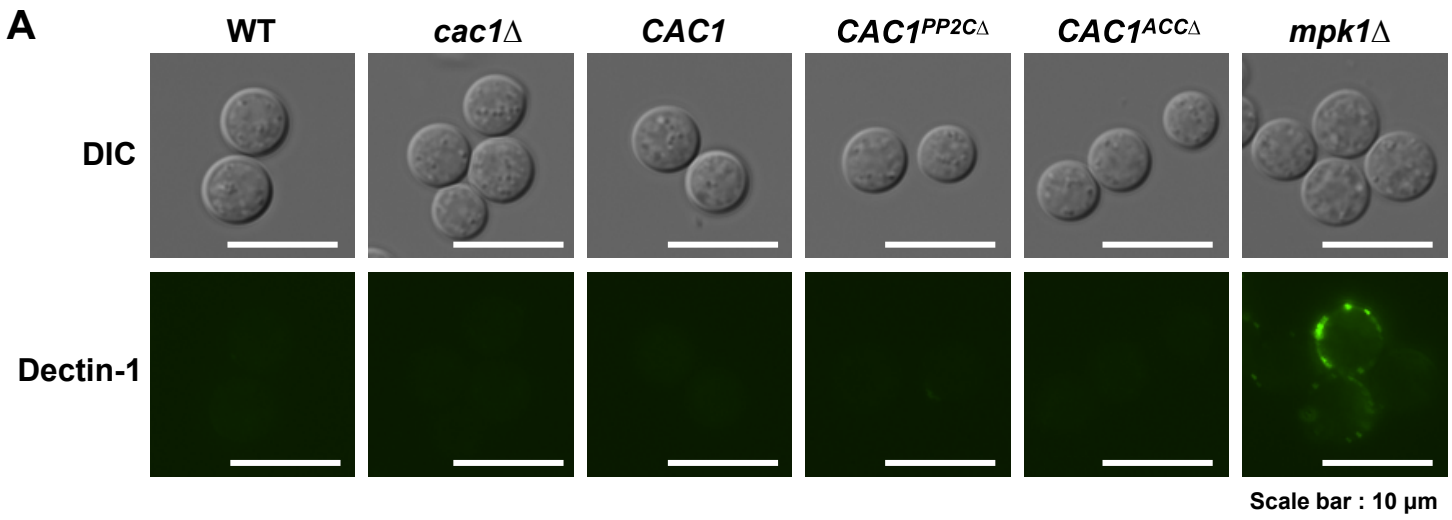

Supplementary Figure 7. Dectin-1 staining revealed that β-1,3-glucans remained masked and undetectable in the *CAC1* and domain deletion strains. A) Dectin-1 staining using soluble human Dectin-1a fused to an IgG1 Fc domain. Indicated strains were cultured for 16 h in liquid YPD at 30°C. The cells were then stained with 15 μg/ml of Fc-hDectin-1a for 1 h, washed twice, and stained with 10 μg/ml of Alexa Fluor 488-conjugated Goat Anti-human IgG in the dark for 1 h. The cells were washed twice and imaged using DIC and fluorescence microscopy. Scale bar, 10 μm.

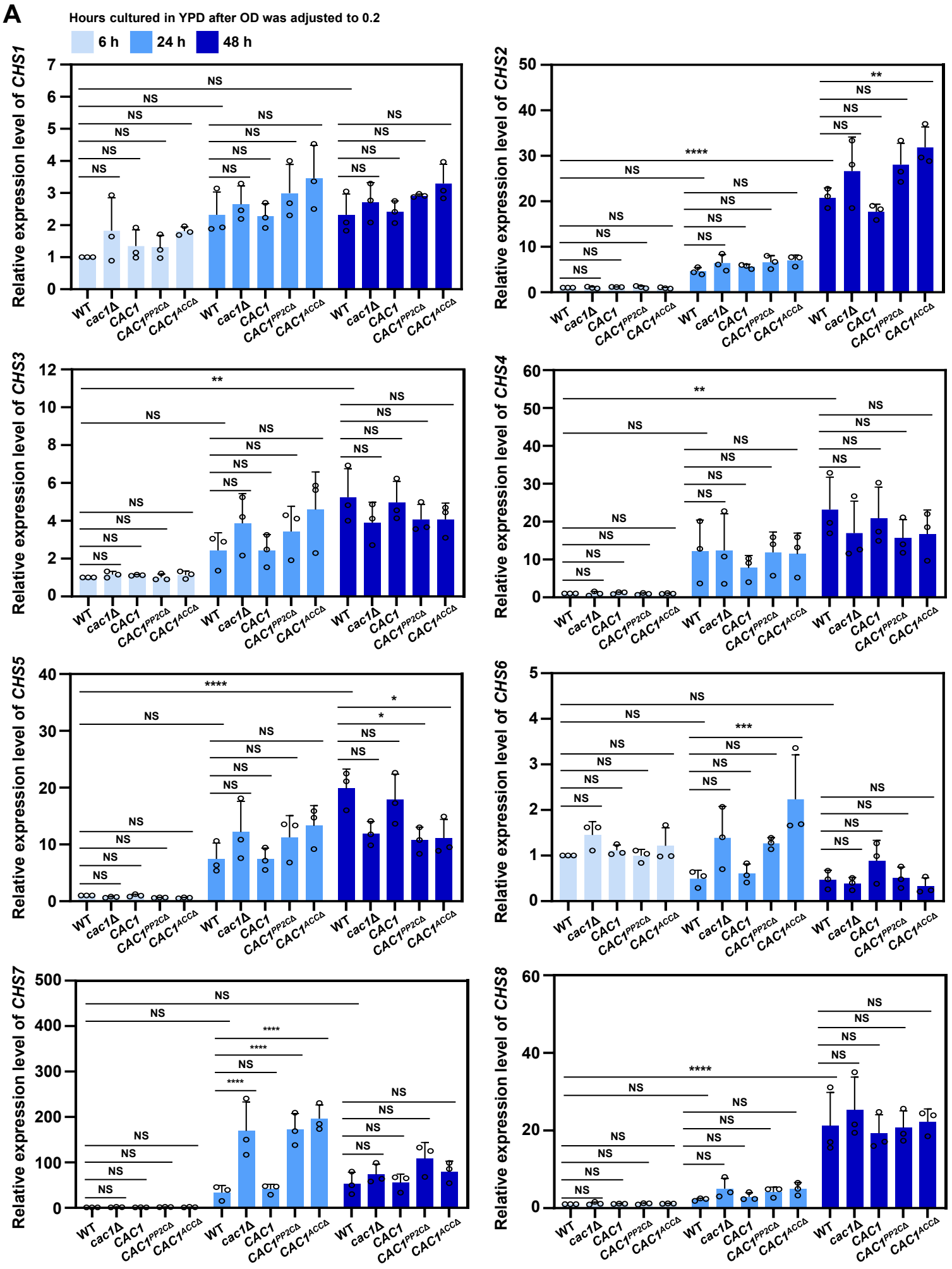
A
Hours cultured in YPD after OD was adjusted to 0.2
6 h
24 h
48 h
Relative expression level of CHS1
Relative expression level of CHS2
Relative expression level of CHS3
Relative expression level of CHS4
Relative expression level of CHS5
Relative expression level of CHS6
Relative expression level of CHS7
Relative expression level of CHS8
WT
cac1Δ
CAC1
CAC1PP2CΔ
CAC1ACCΔ

Continued

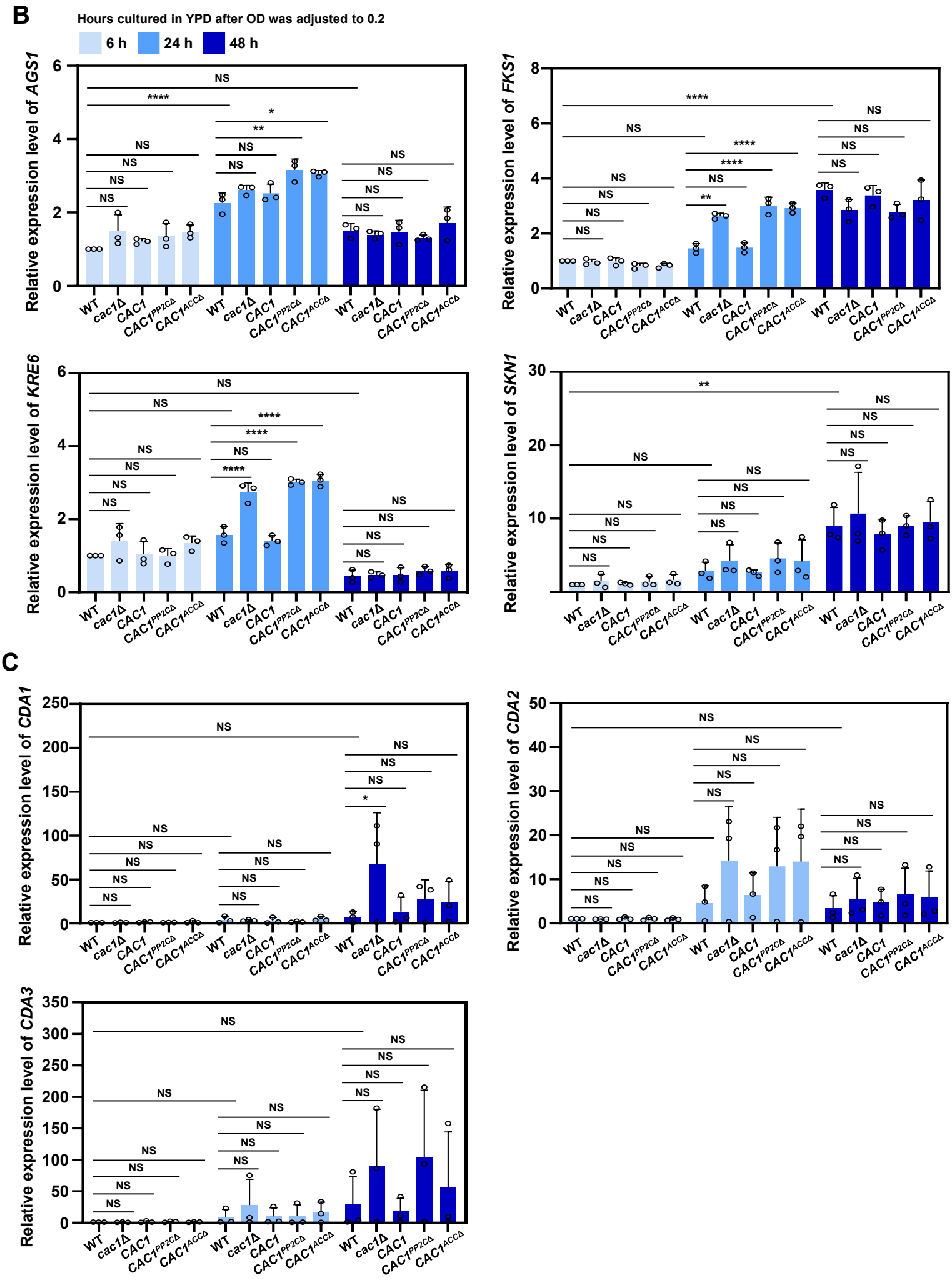
B
Hours cultured in YPD after OD was adjusted to 0.2
6 h
24 h
48 h
Relative expression level of AGS1
Relative expression level of FKS1
Relative expression level of KRE6
Relative expression level of SKN1
C
Relative expression level of CDA1
Relative expression level of CDA2
Relative expression level of CDA3
WT
cac1Δ
CAC1
CAC1PP2CΔ
CAC1ACCΔ
NS
*
**
****

Continued

Supplementary Figure 8. Expression of genes involved in cell wall remodeling. Quantitative RT-PCR was performed using total RNA of each strain under nutrient rich conditions. The cells were cultured for 16 h in liquid YPD at 30°C, synchronized to OD_{600nm} of 0.2, and incubated at 30°C for 6, 24, or 48 h. (A) The expression levels of chitin synthase genes (*CHS1*, *CHS2*, *CHS3*, *CHS4*, *CHS5*, *CHS6*, *CHS7,* and *CHS8*) were measured in WT, *cac1*Δ, *CAC1*, $CAC1^{PP2C\Delta}$, and $CAC1^{ACC\Delta}$ strains. (B) The expression levels of *AGS1*, *FKS1*, *KRE6*, and *SKN1* were measured in the indicated strains. (C) The expression levels of chitin deacetylases (*CDA1*, *CDA2*, and *CDA3*) were measured in the indicated strains. For all genes, three biological replicates were performed with three technical replicates each, and relative transcript levels were calculated using the $2^{-\Delta\Delta Ct}$ method. Error bars indicate SEM, and statistical analysis was performed by one-way ANOVA multiple comparisons with Tukey's multiple comparison test (*, $P < 0.05$; **, $P < 0.01$; ***, $P < 0.001$; ****, $P < 0.0001$; NS, not significant).

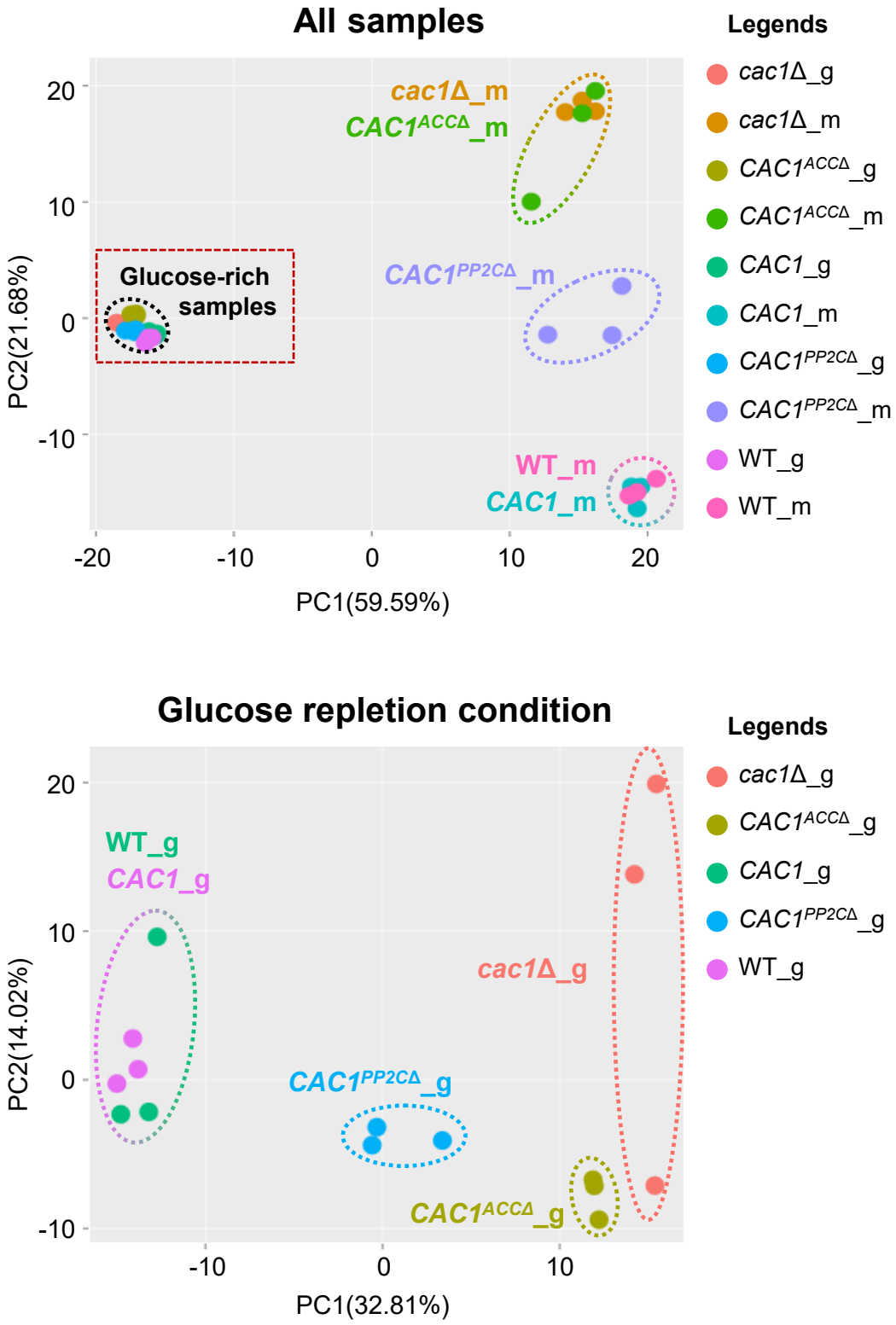

Supplementary figure 9. Principal component analysis of transcriptome profiles across glucose-rich and minimal media conditions. PCA was performed using the R package *debrowser* to visualize transcriptomic similarities and differences among *C. neoformans* strains, including wild-type (WT), *cac1*Δ, complemented strain (*CAC1*), and domain-deletion mutants (*CAC1*$^{PP2C\Delta}$ and *CAC1*$^{ACC\Delta}$). Each dot represents an individual biological replicate. Samples grown in minimal medium (m) and glucose-rich medium (g) (bottom) are shown.

A

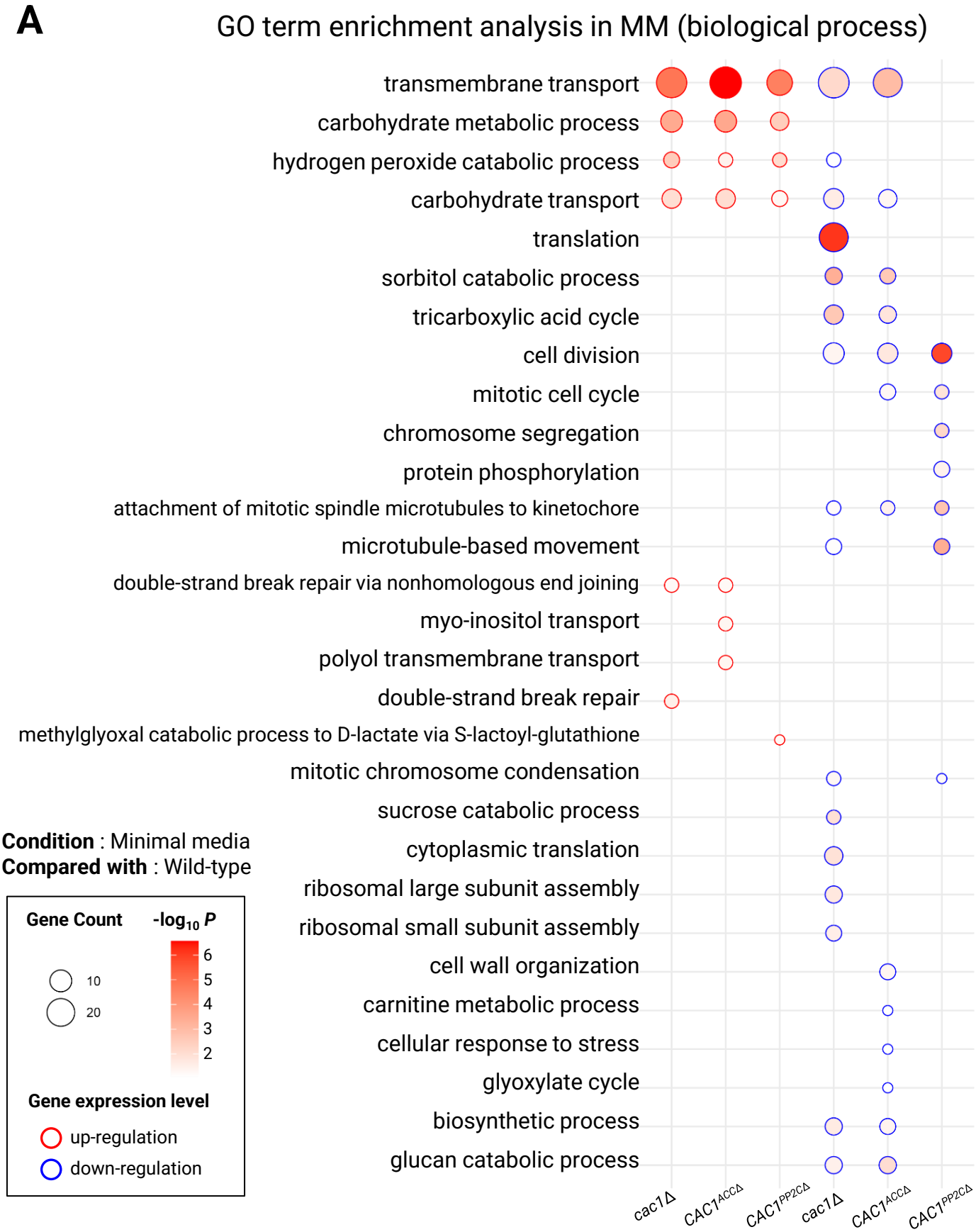
GO term enrichment analysis in MM (biological process)
transmembrane transport
carbohydrate metabolic process
hydrogen peroxide catabolic process
carbohydrate transport
translation
sorbitol catabolic process
tricarboxylic acid cycle
cell division
mitotic cell cycle
chromosome segregation
protein phosphorylation
attachment of mitotic spindle microtubules to kinetochore
microtubule-based movement
double-strand break repair via nonhomologous end joining
myo-inositol transport
polyol transmembrane transport
double-strand break repair
methylglyoxal catabolic process to D-lactate via S-lactoyl-glutathione
mitotic chromosome condensation
sucrose catabolic process
cytoplasmic translation
ribosomal large subunit assembly
ribosomal small subunit assembly
cell wall organization
carnitine metabolic process
cellular response to stress
glyoxylate cycle
biosynthetic process
glucan catabolic process
cac1Δ
CAC1ACCΔ
CAC1PP2CΔ
cac1Δ
CAC1ACCΔ
CAC1PP2CΔ
Condition : Minimal media
Compared with : Wild-type
Gene Count
-log10 P
10
20
6
5
4
3
2
Gene expression level
up-regulation
down-regulation

Continued

B

GO term enrichment analysis in MM (cellular component)

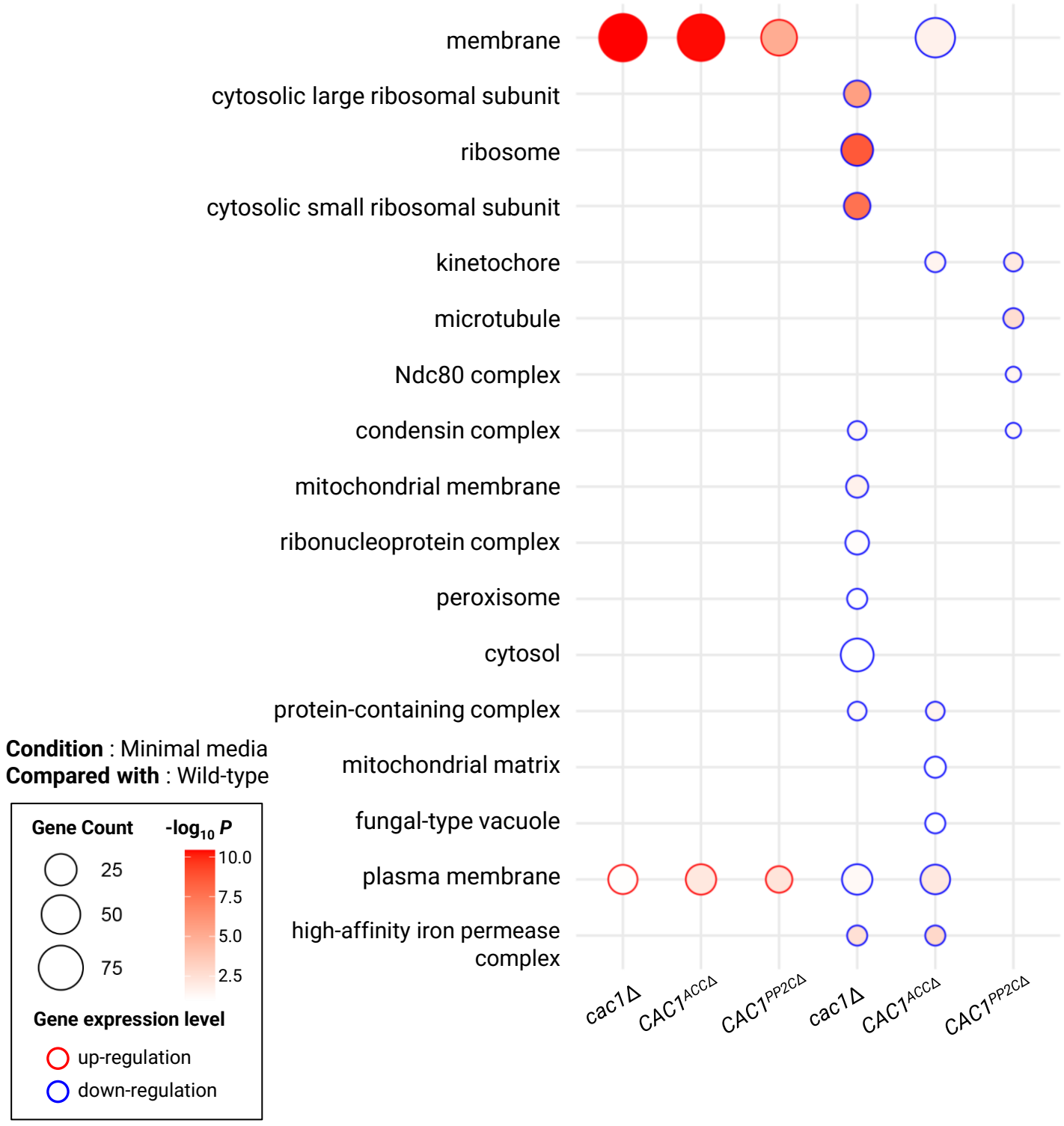

Continued

C

GO term enrichment analysis in MM (molecular function)

Condition : Minimal media
Compared with : Wild-type

Gene Count
10
20

-log$_{10}$ *P*
8
6
4
2

Gene expression level
up-regulation
down-regulation

Continued

D

GO term enrichment analysis in MMG (biological process)

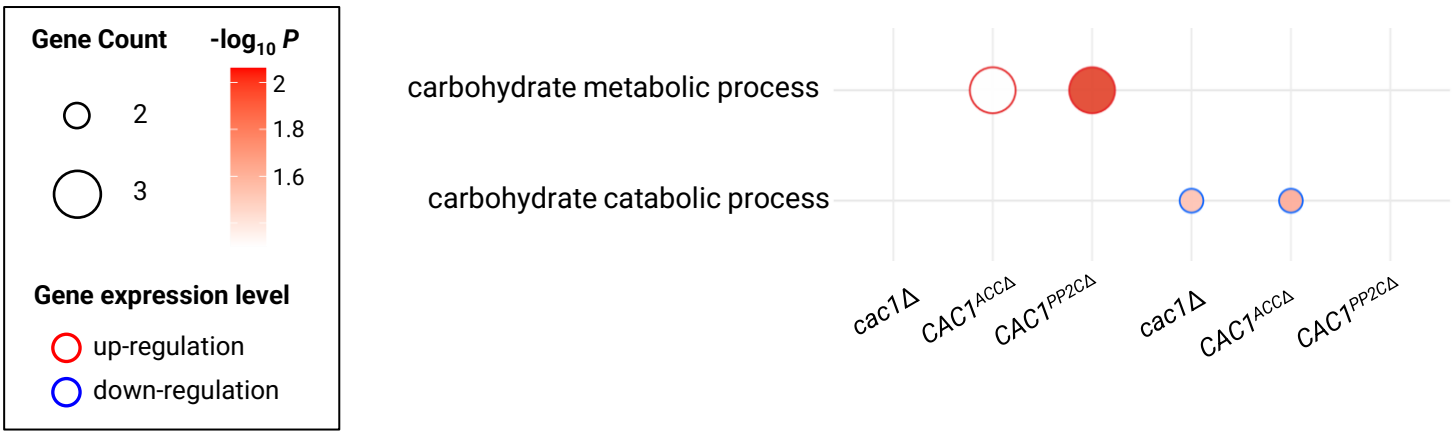

E

GO term enrichment analysis in MMG (cellular component)

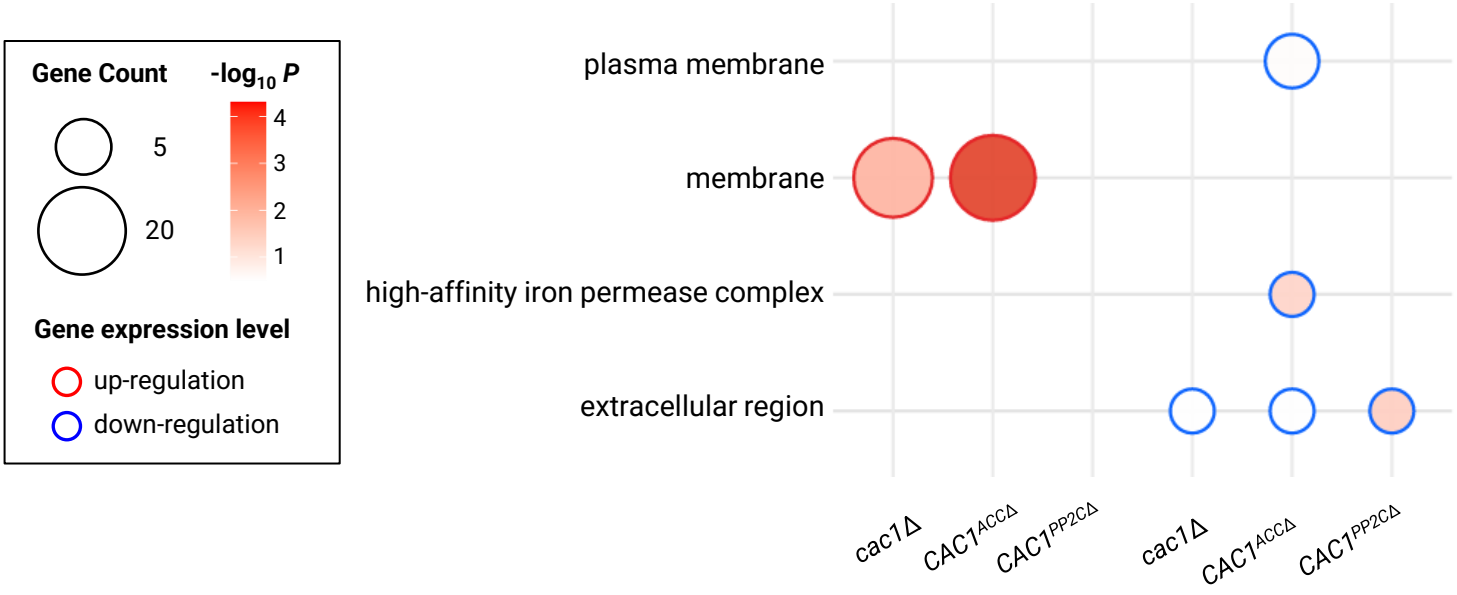

F

GO term enrichment analysis in MMG (molecular function)

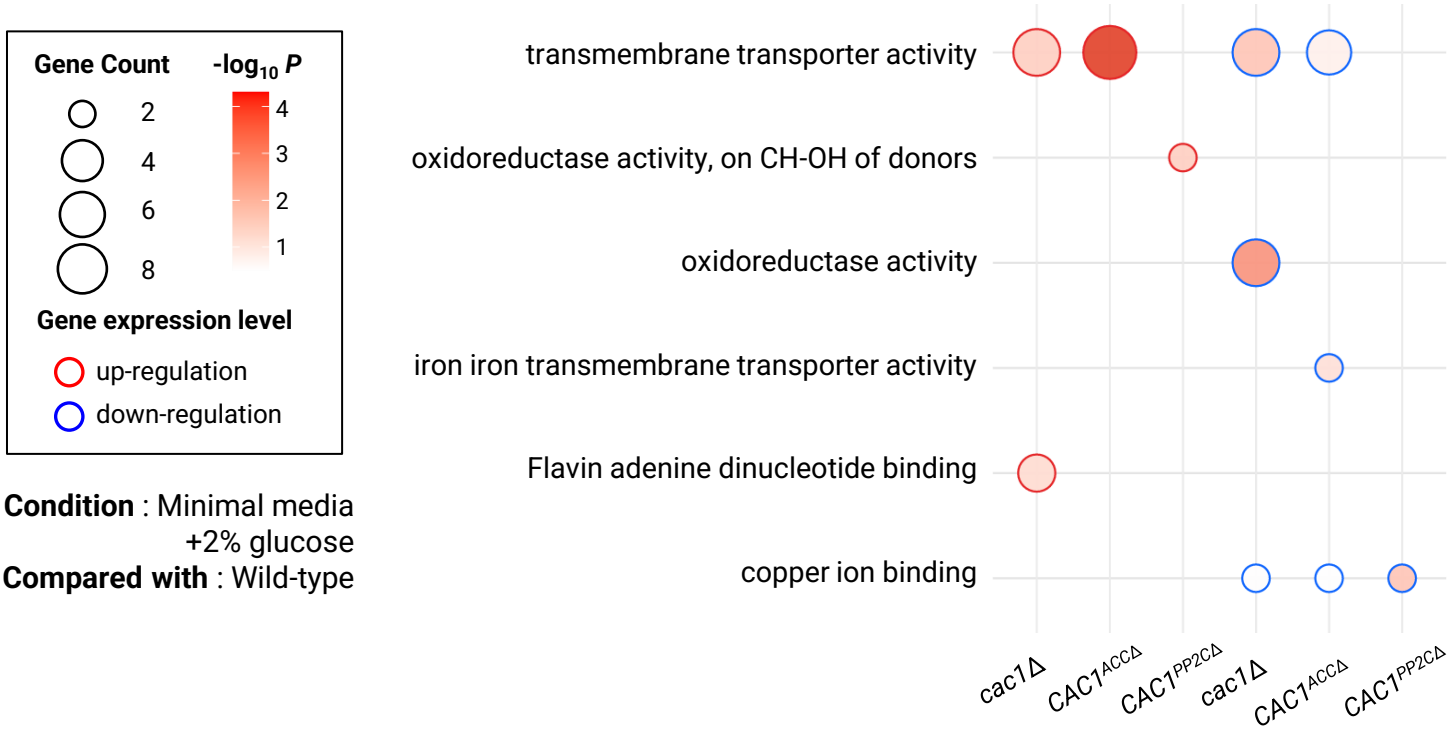

Condition : Minimal media +2% glucose
Compared with : Wild-type

Continued

Supplementary figure 10. GO term enrichment analysis of differentially expressed genes in *CAC1* domain-deletion mutants. (A,D) Biological process, (B,E) cellular component, (C,F) molecular function terms. Bubble plots show Gene Ontology (GO) enrichment results for upregulated and downregulated genes in *cac1*Δ, *CAC1*$^{ACC\Delta}$, and *CAC1*$^{PP2C\Delta}$ strains. (A-C) is for minimal media (MM), and (D-F) is for minimal media + 2% glucose condition (MMG). The color gradient of the bubbles represents the $-\log_{10} P$, while bubble size indicates the number of genes associated with each GO term. Red bubbles denote enriched terms among upregulated genes, and blue bubbles denote those among downregulated genes.

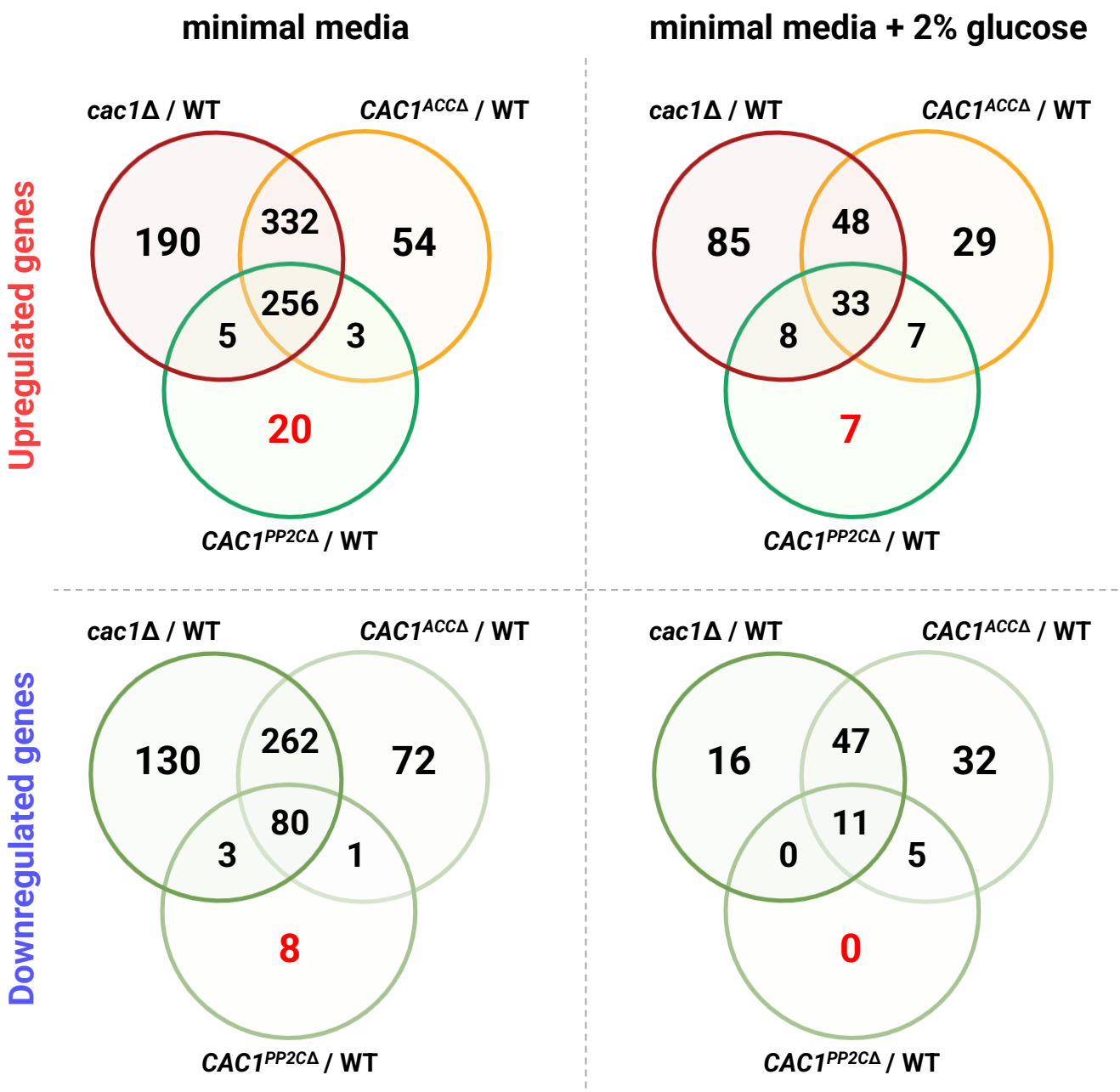

Supplementary figure 11. Venn diagram analysis of differentially expressed genes in *CAC1* domain-deletion mutants. Venn diagrams show the overlap of significantly upregulated (top) and downregulated (bottom) genes among the *CAC1* full deletion mutant (*cac1*Δ), the PP2C domain deletion mutant (*CAC1*$^{PP2C\Delta}$), and the adenylyl cyclase catalytic domain deletion mutant (*CAC1*$^{ACC\Delta}$). Analyses were performed separately for cells grown in minimal medium (left) and glucose-rich medium (right). Differential expression was defined by $|\log_2 FC| \geq 1$ and adjusted $P < 0.05$. The numbers indicate the count of shared or unique differentially expressed genes between strains under each condition.

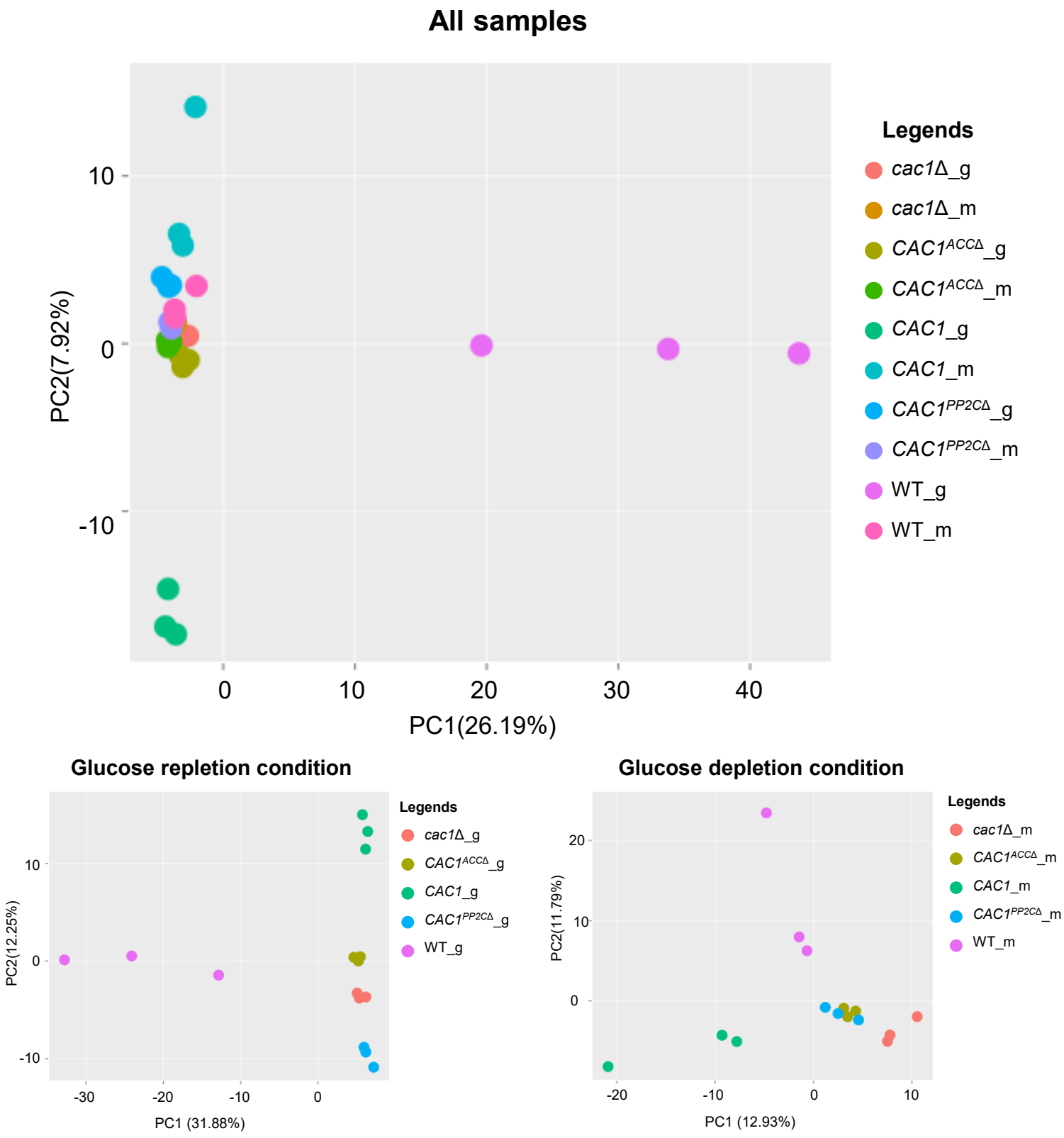

Supplementary figure 12. Principal component analysis of transcriptome profiles across glucose-rich and minimal media conditions. PCA was performed using the R package *debrowser* to visualize phosphoproteomic similarities and differences among *C. neoformans* strains, including wild-type (WT), *cac1*Δ, complemented strain (*CAC1*), and domain-deletion mutants ($CAC1^{PP2C\Delta}$ and $CAC1^{ACC\Delta}$). Each dot represents an individual biological replicate. Samples grown in minimal medium (m) and glucose-rich medium (g) (bottom) are shown.

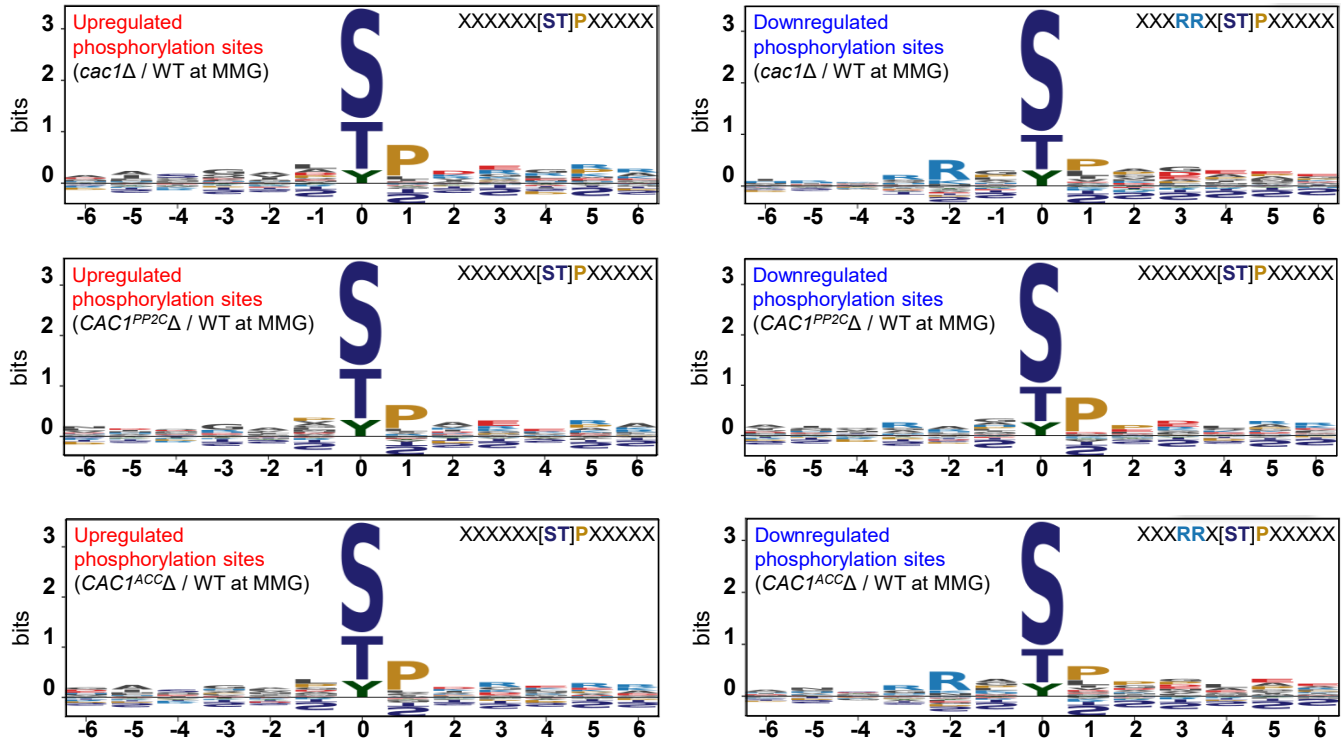

Supplementary figure 13. Sequence motif analysis of differentially regulated phosphorylation sites in *C. neoformans* Cac1 mutants under MMG condition. Phosphorylation motifs were analyzed for sites that were upregulated (left, red labels) or downregulated (right, blue labels) in *cac1Δ*, *CAC1*$^{PP2C\Delta}$, and *CAC1*$^{ACC\Delta}$ strains compared with wild type (WT) under minimal medium supplemented with 2% glucose (MMG). Sequence logos were generated to represent the amino acid frequencies surrounding phosphorylated serine/threonine residues (position 0). Distinct enrichment patterns are observed between upregulated and downregulated sites, including proline-directed motifs ([S/T]P) in upregulated sites and basic residue-enriched motifs (Rxx[S/T]) in downregulated sites.

Supplementary Table 1. List of strains used in this study.

Strain	Genotype	Parent	Reference
H99	*MAT*α		(1)
YSB5650	*MAT*α CNAG_03202::NAT-STM #159 (*cac1*Δ)	H99	(2)
YSB7883	*MAT*α *cac1*Δ::*CAC1* - NEO	YSB5650	This study
YSB7885	*MAT*α *cac1*Δ::*CAC1* PP2CΔ - NEO	YSB5650	This study
YSB8184	*MAT*α *cac1*Δ::*CAC1* ACCΔ - NEO	YSB5650	This study
YSB3814	*MAT*α CNAG_04514::NAT-STM #240 *(mpk1*Δ)	H99	(3)
AI167	*MAT*α CNAG_03658::NAT (*ena1*Δ)	H99	(4)
Escherichia coli BL21 (DE3)	λ(DE3), T7 RNA polymerase	*Escherichia coli* B	(5)

1. Perfect JR, Ketabchi N, Cox GM, Ingram CW, Beiser CL. 1993. Karyotyping of *Cryptococcus neoformans* as an epidemiological tool. *J Clin Microbiol* 31:3305-9.
2. Jin JH, Lee KT, Hong J, et al. 2020. Genome-wide functional analysis of phosphatases in the pathogenic fungus *Cryptococcus neoformans. Nat Commun* 11, 4212.
3. Lee KT, So YS, Yang DH, et al. 2016. Systematic functional analysis of kinases in the fungal pathogen *Cryptococcus neoformans*. *Nat Commun* 7, 12766.
4. Idnurm A, Walton FJ, Floyd A, Reedy JL, Heitman J. 2009. Identification of *ENA1* as a virulence gene of the human pathogenic fungus *Cryptococcus neoformans* through signature-tagged insertional mutagenesis. *Eukaryot Cell* 8.
5. Studier, F. W., and Moffatt, B. A. 1986. Use of bacteriophage T7 RNA polymerase to direct selective high-level expression of cloned genes. *J. Mol. Biol*. 189, 113–130.

Supplementary Table 2. List of primers used in this study.

Primer Name	Sequence (5' to 3')	Comment
B11623	CGGCCGCCAGTGTGATGGATAAAAG AGCAGGATGGGAAG	*CAC1* complementation primer LP
B11624	CAAGGGCGAATTCTGCAGATGTCTG AACTTGAAGGGAATG	*CAC1* complementation primer RP
B11660	CAGCTGTAATAATCTTCGATGTTGGA TTGTTAAC	*CAC1* split primer MRP
B11661	ATCGAAGATTATTACAGCTGGGCCA TAC	*CAC1* split primer MLP
B11729	CATTGACAATCTTGCCATGATGGTCA TGGTGGTG	*CAC1* PP2C domain deletion LP
B11730	CATTCACCACCATGACCATCATGGC AAGATTGTC	*CAC1* PP2C domain deletion RP
B11731	CCGACTCCAGCAAGAGTTGAAGAGG GAAGTTATGG	*CAC1* ACC domain deletion LP
B11732	CCATAACTTCCCTCTTCAACTCTTGC TGGAGTCGG	*CAC1* ACC domain deletion RP
B11771	GTCATTGGTTCTTTTGCGG	*CAC1* sequencing primer 1
B11772	CCTCTAAATCACCACCATTCAC	*CAC1* sequencing primer 2
B11773	GCAGGTTTATCGCCCTCTAC	*CAC1* sequencing primer 3
B11774	CGGACAACAACAACATCGTC	*CAC1* sequencing primer 4
B11775	GACGAATCTGCCATCTGAG	*CAC1* sequencing primer 5
B11776	TGCTGTGGTTTACCTCGTG	*CAC1* sequencing primer 6
B11777	GTGTCTTTCCAATCTGTTGC	*CAC1* sequencing primer 7
B11778	GTGGGGAGGATTGAAAAC	*CAC1* sequencing primer 8
B11779	GGACTGTAAAAGATGCCTCG	*CAC1* complementation screening primer LP
B11780	CTTGCGTTTCCGACAATG	*CAC1* complementation screening primer RP
B679	CGCCCTTGCTCCTTCTTCTATG	*ACT1* qRT primer qLP
B680	GACTCGTCGTATTCGCTCTTCG	*ACT1* qRT primer qRP
B15938	CACCCTTTGGAAGTTGTGG	*LAC1* qRT primer qLP
B15939	TGATAATTGCAGAGTACCG	*LAC1* qRT primer qRP
B15950	TCCAGCCTTGGCTTCACTAT	*CAP10* qRT primer qLP
B15951	GGCATCGAGCATAGCCTTAG	*CAP10* qRT primer qRP
B8684	GCTATTAGAGGCTACAAGCG	*CAP59* qRT primer qLP
B8685	GGGTGAACAACCTATCGTG	*CAP59* qRT primer qRP
B8643	ACGCTATGAACGAAGAGGC	*CAP60* qRT primer qLP
B8644	GGAGTGAAAACAGAGTTGGG	*CAP60* qRT primer qRP
B8645	CAAGGAAAGGGCATTCAGAG	*CAP64* qRT primer qLP
B8646	TCAGAAAGCATTGCCTGG	*CAP64* qRT primer qRP
B23102	CCCACTCCCGGTCTCAAATA	*BZP4* qRT primer qLP
B23103	CAGTAGGCGAGACAGGTGAT	*BZP4* qRT primer qRP
B23106	TGGGTCCGAGAACATTGTGT	*GAT201 qRT primer qLP*

B23107	CTGCCTCCAATCTCGCTTTC	*GAT201* qRT primer qRP
B23108	CGCCTAGACCTTCACTCGAT	*PDR802* qRT primer qLP
B23109	CTTTGGTGGCAGAAAGGGAC	*PDR802* qRT primer qRP
B22028	AGGGTGAAAGAGAGGGAAC	*ADA2* qRT primer qLP
B22029	GCTTTTTTGCGTTGCTGG	*ADA2* qRT primer qRP
B15946	CAGAATGCAAGCCAGAATCA	*YAP1* qRT primer qLP
B15947	GCGTTCATGCTGTTGTTGTT	*YAP1* qRT primer qRP
B9368	CCGCCGGTATTGTTAAGATG	*CHS1* qRT primer qLP
B9369	CCCAAAAGTACCGCTATCCA	*CHS1* qRT primer qRP
B9370	GCAACTTGGTGATGGATGTG	*CHS2* qRT primer qLP
B9371	AGTACCGCATGCTGTCCATT	*CHS2* qRT primer qRP
B9372	CCAAGGGTTTTCGGACTACA	*CHS3* qRT primer qLP
B9373	TCACGATAATGCCAGAGACG	*CHS3* qRT primer qRP
B9374	ACGCCCATCATATTCTGCTC	*CHS4* qRT primer qLP
B9375	TTCTCCTTGACGACCATTCC	*CHS4* qRT primer qRP
B9376	CAAGGGTGGTGGAAGAAGAA	*CHS5* qRT primer qLP
B9377	ATAACCTGATCCTGCCCAGTC	*CHS5* qRT primer qRP
B9378	GGCCCCCTCTTATGACTACC	*CHS6* qRT primer qLP
B9379	TGATCTTCCCCTTGGAGTTG	*CHS6* qRT primer qRP
B9380	CGTTCCTTACGACTGATCCA	*CHS7* qRT primer qLP
B9381	TCTCAAGAAATCGGCTCCTG	*CHS7* qRT primer qRP
B12142	ACGTTTGCGTCCTTCTTGAC	*CHS8* qRT primer qLP
B12143	AATGCGACAATCTCACCACA	*CHS8* qRT primer qRP
B14791	CTGCCGCAGCTATTTTTAGG	*AGS1* qRT primer qLP
B14792	CGATGATGGGGAAGTAGGAA	*AGS1* qRT primer qRP
B14793	TCGAATGTCCCCTAACCAAG	*FKS1* qRT primer qLP
B14794	CAAGTCGAGTTGAGCAGCAA	*FKS1* qRT primer qRP
B14795	TGGACGTTGGTGTTTTCAGA	*SKN1* qRT primer qLP
B14796	CCAGTGGGCCAATAGTGAAT	*SKN1* qRT primer qRP
B14799	GAAGACCATCCAGGTCCAGA	*KRE6* qRT primer qLP
B14800	GGGAGACTTCTCCTCGGTTC	*KRE6* qRT primer qRP
B11629	CTGACTCTACTGTGGCCCTC	*CDA1* qRT primer qLP
B11630	TCACCATCGCCGATTATCCA	*CDA1* qRT primer qRP
B11631	GTGATTGGACCGGTGTGAAC	*CDA2* qRT primer qLP
B11632	CACTGGTTTGCAAGCCGATA	*CDA2* qRT primer qRP
B11633	TGCCAAATGTTCCAGTAGCT	*CDA3* qRT primer qLP
B11634	TCTTTCACCGATCAATGCCG	*CDA3* qRT primer qRP
PP2C_5BamHI	CG GGATCC TTG GGCTCCATTGACAATCTTGCCATG	CAC1 PP2C pET cloning primer 5'
PP2C_3XhoI	CCCTCGAGTCAGAACAAATCAGACA CATTCACCAC	CAC1 PP2C pET cloning primer 3'

Supplementary Note 1: Detailed methods for expression and purification of the PP2C domain.

When the OD_{600} reached 0.6~0.8 after 6 h, cells were induced with 0.5 mM IPTG (isopropyl 1-thio-ß-D-galactopyranoside) and 2 mM $MnCl_2$ at 17°C overnight. The cells were harvested in 3000 rpm 20 min with low-speed centrifuge and then sonicated (3 seconds on, 5 seconds off, at 60% amplitude, 5 min) in lysis buffer consisting of 25 mM Tris-HCl pH 8.0, 300 mM NaCl, 10 % glycerol, 30 mM imidazole, 2 mM $MnCl_2$. After centrifuge at 13000 rpm for 2 h using high-speed centrifuge, supernatant was filtered 0.45 μm 47 mm membrane disks (1215676; GVS Life Sciences, Italy). His tagged proteins were then purified using nickel-affinity chromatography (His60 Ni Superflow Resin) by elution buffer consisting of 25 mM Tris-HCl pH 8.0, 300 mM NaCl, 10% glycerol, 300 mM imidazole, 2 mM $MnCl_2$. PP2C domain was then concentrated using Vivaspin 20 centrifuge concentrator with a molecular cut-off of 30 kDa and further purified by size exclusion chromatography on Superdex 200 Increase gel filtration column (Cytiva, USA) with SEC buffer containing 20 mM HEPES-NaOH (pH 8.0), 300 mM NaCl, 2 mM $MnCl_2$. Proteins were stored in the deep freezer after mixing with 100% glycerol in a ratio of 20% and aliquoted in 200 μl until assay.

Supplementary Note 2: Detailed methods for phospho-amino acid dephosphorylating and catalytic activity assay.

For phospho-amino acid and dephosphorylating assay, the standard curve was obtained at the 620 nm by spectrometer, plate reader CLARIOstar Plus (BMG Labtech, Germany) based on quantification of the green complex formed between Malachite green and molybdate with different free orthophosphate concentration from 0-40 μM. The amount of dephosphorylated free phosphate was measured with 10 μM recombinant proteins at RT for 30 min in a 20 μl of the working reagent to 80 μl of sample protein solution. The assay was ended by the addition of the working reagent. For dephosphorylation catalytic activity assay, the standard curve was obtained from the excitation/emission at 360 nm/460 nm wavelength plate reader CLARIOstar Plus with different DiFMU concentration from 0-100 μM. Assay towards 0-200 μM DiFMUP were conducted using 40 μg purified recombinant PP2C proteins at RT for each 3 min (incubate protected from light) in a 50 μl reaction mixture buffer and 50 μl of sample protein solution.

Supplementary Note 3: Detailed methods for gene expression analysis using quantitative RT-PCR.

To prepare samples for RNA extraction of melanin-regulating genes, cells were cultured in 50 ml of YPD for 16 h at 30°C. Then, OD_{600} was adjusted to 0.2, and when cells reached OD_{600} of 0.8, 10 ml of sample was spun down, frozen in liquid nitrogen, and lyophilized as basal sample. The remaining cells were washed three times with sterile PBS, resuspended in liquid yeast nitrogen base (YNB) medium without glucose, and incubated at 30°C for 2 h. The cells were then spun down, frozen in liquid nitrogen, and lyophilized. For capsule related genes, the basal sample was prepared in the same method, and the remaining cells were washed three times with sterile PBS, resuspended in 10% FBS for 2 or 6 h. The cells were then spun down, frozen in liquid nitrogen, and lyophilized. To prepare samples for RNA extraction of chitin synthesis-related genes, the cells were cultured in 50 ml of YPD for 16 h at 30°C, OD_{600} adjusted to 0.2, and incubated in YPD at 30°C. Samples were then collected 6, 24, or 48 h later. Each sample was spun down, frozen in liquid nitrogen, and lyophilized. For RNA extraction, lyophilized samples were homogenized with 3 mm glass beads, and total RNA was extracted using an RNA extraction kit (iNtRON Biotechnology, South Korea). RNA concentration was then measured, and 5,000 ng of total RNA was used to synthesize cDNA using reverse transcriptase (ThermoFisher Scientific, USA). qRT-PCR was then performed using CFX96 (Bio-Rad Laboratories, USA) using primers designed for each target gene and TB Green (ThermoFisher Scientific, USA). Unless otherwise specified as "normalized to *ACT1*," transcript levels were calculated by the ΔΔCt method with *ACT1* as the reference gene. For targets with very low basal expression – specified by "normalized to *ACT1*" – we report ΔCt = Ct(target) – Ct(*ACT1*) per sample because ΔΔCt produced unstable fold changes. Statistical analysis was performed by one-way ANOVA or student *t*-test, which is specified in each figure legend. The relative gene expression was then visualized using Prism 10.4.

Supplementary Note 4: Detailed methods for histochemistry, immune cell, and cytokine analyses.

For tissue staining, lungs were obtained from mice on day 14 after infection and fixed in 3.7% formalin solutions. After complete fixation, the tissue was dehydrated and clarified using xylene before being embedded in paraffin blocks. Tissue sections with a thickness of 5 μm were cut and stained with Grocott's Methenamine Silver (GMS) Stain Kit (ab287884; Abcam, UK), following the manufacturer's protocol. The slide images were taken with a Primostar 3 (ZEISS, Germany) at a final 400× magnification.

For immune cell analysis, immune cells were isolated from the lungs of the infected mice to identify the population of each immune cell. The cells were washed with PBS and Fcγ receptors were blocked by Anti-CD16/CD32 (14-0161; Invitrogen, USA). Subsequently, the cells were stained with surface markers, FITC-conjugated anti-CD3 (11-0032; Invitrogen) PE-Cy7-conjugated anti-CD4 (25-0041; Invitrogen), PerCP-Cy5.5-conjugated anti-CD8 (45-0081; Invitrogen), APC-conjugated anti-CD19 (17-0193; Invitrogen), FITC-conjugated anti-F4/80 (11-4801; Invitrogen), FITC-conjugated anti-MHC Class II (11-5321; Invitrogen), and APC-conjugated anti-CD11b (17-0112; Invitrogen). Stained cells were analyzed using BD FACSymphony A3 and FlowJo V10 software.

For cytokine analysis, the infected mice were euthanized to collect serum. IFN-γ and IL-4 levels in the serum were quantified using ELISA kits (IFN-γ: 88-7314, IL-4: 88-7044; Invitrogen), following the manufacturer’s instructions. Briefly, 96-well immunoplates (32296; SPL, South Korea) were coated with capture antibodies and incubated with overnight at 4°C. After washing with PBS containing 0.05% Tween-20 (PBST), plates were blocked with 1% BSA in PBS for 1 h at room temperature. Serum samples and recombinant cytokine standards were added in duplicate and incubated for 2 h at room temperature. Plates were then incubated

with biotinylated detection antibodies, followed by streptavidin-HRP conjugate. After extensive washing, TMB substrate solution was added, and the reaction was stopped with 2 N H_2SO_4. Absorbance was measured at 450 nm using a microplate reader (SpectraMax, Molecular Devices, USA).

Supplementary note 5: Detailed methods for transmission electron microscopy.

Cells were grown overnight at 30℃ in YPD broth and synchronized to OD_{600} = 0.2 in liquid YPD medium and then further incubated until they reached $OD6_{00}$ = 0.8. The harvested cells were fixed with 2% paraformaldehyde and glutaraldehyde fixation solution and sent into Yonsei Biomedical Research Institute, Yonsei University College of Medicine for TEM analysis. Cells were fixed for 12 h in 2% glutaraldehyde + 2% paraformaldehyde in 0.1 M phosphate buffer (pH 7.4), rinsed in the same buffer, and post-fixed in 1% OsO_4 (0.1 M phosphate buffer) for 2 h. Samples were dehydrated through a graded ethanol series (50, 60, 70, 80, 90, 95, 100%, 10 min each), infiltrated with propylene oxide for 10 min, and embedded in Poly/Bed 812. Polymerization was carried out at 70℃ for 12 h in an EM oven. Blocks were trimmed and sectioned on an Ultramicrotome (UC7). Semithin sections (200 nm) were stained with toluidine blue for light-microscopy orientation. The regions of interest were then sectioned at 80 nm, mounted on copper grids, and contrast-stained with 5% uranyl acetate (20 min) followed by 3% lead citrate (7 min). Imaging was performed on a Hitachi HT7800 TEM operated at 100 kV equipped with an RC camera. For thickness measurement, five positions were measured and averaged for each cell (8 cells per strain) at 150,000x magnification using ImageJ. For quantification of inner wall density, images were inverted to reverse black and white contrast, and the mean intensity of the inner-wall region was measured for each strain at 150,000x magnification (8 cells per strain). Statistics were performed by one-way ANOVA with Bonferroni's multiple comparisons (****, $P < 0.0001$; NS, not significant).

Supplementary note 6: Detailed methods for LC-MS analysis.

Quantitative LC/MS/MS was performed using an EvoSep One UPLC coupled to a Thermo Orbitrap Astral high-resolution accurate mass tandem mass spectrometer. Briefly, each sample loaded EvoTip was eluted onto a 1.5 µm EvoSep 150um ID x 15cm performance column using the SPD30 gradient at 55°C. Data collection on the Orbitrap Astral mass spectrometer was performed in a data-independent acquisition (DIA) mode of acquisition with a r=240,000 (@ m/z 200) full MS scan from m/z 380-1080 in the OT with a target AGC value of 4e5 ions. Fixed DIA windows of 5 m/z from m/z 380 to 1080 DIA MS/MS scans were acquired in the Astral with a target AGC value of 5e4 and a max fill time of 8 ms. HCD collision energy setting of 27% was used for all MS2 scans. The total analysis cycle time for each sample injection was approximately 40 min. Following 34 total UPLC-MS/MS analyses (30 experimental samples and 4 internal quality control samples), data were imported into Spectronaut (Biognosis), and individual LCMS data files were aligned based on the accurate mass and retention time of detected precursor and fragment ions. Relative peptide abundance was measured based on MS2 fragment ions of selected ion chromatograms of the aligned features across all runs. The MS/MS data was searched against a *Cryptococcus neoformans* H99 database (downloaded in 2024), a common contaminant/spiked protein database (bovine albumin, bovine casein, yeast ADH, etc.), and an equal number of reversed-sequence "decoys" for false discovery rate determination. A library was created using only LC-MS data files collected within this study. Database search parameters included fixed modification on Cys (carbamidomethyl) and variable modification on Met (oxidation), Protein N-term (acetyl), and Ser/Thr/Tyr (phos). Full trypsin enzyme rules were used along with 10 ppm mass tolerances on precursor ions and 20 ppm on product ion. Spectral annotation was set at a maximum 1% peptide false discovery rate based on q-value calculations. Note that peptide homology was addressed using razor rules in which a peptide matched to multiple different proteins was exclusively assigned to the protein

that has more identified peptides. The output raw peptide intensity values from the Spectonaut detection software were noted. At this stage, any peptide that was not detected a minimum of 2 times across all of the samples and not detected in at least 50% of one of the biological groups was removed from further analysis. For remaining peptides, any missing data values were imputed using the following rules: 1) if less than 50% of signals were missing within a group, a randomized value near the average of the remaining values was calculated, or 2) if >50% of the signals were missing within the group, a randomized intensity within the bottom 1% of the detectable signals was used. Next, non-phosphorylated peptides and phosphopeptides which did not pass a 75% confidence of localization were removed from the analysis. The remaining phosphopeptides were then subjected to a robust mean normalization in which the highest and lowest 10% of the phosphopeptide signals were ignored and the average value of the remaining phosphopeptides was used as the normalized factor across all samples. We then summed all of the same precursor states for the same phosphopeptide (ie. different charge states) into a single modified phosphopeptide value and calculated the percent coefficient of variation across each group. Following database searching and peptide scoring using a library-based Spectronaut search, the data was annotated at a 1% peptide false discovery rate. A total of 103,664 phosphopeptides were identified in the dataset corresponding to 3,434 phosphoproteins.

Supplementary note 7: Detailed methods for bioinformatics analysis of transcriptome and phosphoproteome.

Raw sequencing reads were subjected to quality control and adapter trimming using Cutadapt v2.4 in Python 3.7.4, employing the specified adapter sequence[1]. Subsequent read processing followed previously established protocols[2]. Cleaned reads were aligned to the *Cryptococcus neoformans* H99 reference genome using Hisat2 v2.2.1, which utilizes the Hisat and Bowtie2 algorithms. Genome annotation files were retrieved from the NCBI FTP repository. Hisat2 was executed with the parameters "-p 30" and "--dta -1," along with default settings. The resulting alignment files were converted and sorted using Samtools v0.1.19, applying "-Sb -@ 8" for file conversion and "-@ 20" for sorting operations[3]. Gene-level expression matrices were generated and further analyzed using the R package IsoformSwitchAnalyzeR[4]. Data quality was evaluated with DEBrowser[5], and DEGs were identified using DESeq2 v1.24[6]. DEGs were defined based on a threshold of a >2-fold change and a P-value <0.05, and visualized using the EnhancedVolcano package in R v4.1.0[7]. For phosphoproteome analysis, the raw phosphopeptide intensity tables were imported into Perseus v1.6.15.0 for statistical analysis[8]. Intensities were first transformed to log scale and normalized by subtracting the median value of each sample to reduce systematic variation across runs. For pairwise comparisons between strains and media conditions, two-sided Student's t-tests were performed in Perseus with permutation-based false discovery rate (FDR) control (FDR <0.05). Significantly altered phosphorylation events were defined using a combined threshold of $|\log_2 > \text{fold change}| > 1$ and P <0.05. Volcano plots were generated via EnhancedVolcano package to visualize differentially phosphorylated peptides. Functional enrichment analysis was conducted for the set of significantly altered phosphoproteins or transcriptome. Gene Ontology (GO) term enrichment was performed using the DAVID[9].

References

1 Kechin, A., Boyarskikh, U., Kel, A. & Filipenko, M. CutPrimers: a new tool for accurate cutting of primers from reads of targeted next generation sequencing. *J Comput Biol* **24**, 1138-1143, doi:10.1089/cmb.2017.0096 (2017).

2 Pertea, M., Kim, D., Pertea, G. M., Leek, J. T. & Salzberg, S. L. Transcript-level expression analysis of RNA-seq experiments with HISAT, StringTie and Ballgown. *Nat Protoc* **11**, 1650-1667, doi:10.1038/nprot.2016.095 (2016).

3 Li, H. *et al.* The Sequence Alignment/Map format and SAMtools. *Bioinformatics* **25**, 2078-2079, doi:10.1093/bioinformatics/btp352 (2009).

4 Vitting-Seerup, K. & Sandelin, A. IsoformSwitchAnalyzeR: analysis of changes in genome-wide patterns of alternative splicing and its functional consequences. *Bioinformatics* **35**, 4469-4471, doi:10.1093/bioinformatics/btz247 (2019).

5 Kucukural, A., Yukselen, O., Ozata, D. M., Moore, M. J. & Garber, M. DEBrowser: interactive differential expression analysis and visualization tool for count data. *BMC Genomics* **20**, 6, doi:10.1186/s12864-018-5362-x (2019).

6 Love, M. I., Huber, W. & Anders, S. Moderated estimation of fold change and dispersion for RNA-seq data with DESeq2. *Genome Biol* **15**, 550, doi:10.1186/s13059-014-0550-8 (2014).

7 EnhancedVolcano: Publication-ready volcano plots with enhanced colouring and labeling (R package version 1.4.0, 2019).

8 Tyanova, S. *et al.* The Perseus computational platform for comprehensive analysis of (prote)omics data. *Nat Methods* **13**, 731-740, doi:10.1038/nmeth.3901 (2016).

9 Dennis, G., Jr. *et al.* DAVID: Database for Annotation, Visualization, and Integrated Discovery. *Genome Biol* **4**, P3 (2003).